Surface modification of lipid nanocapsules with polysaccharides: From physicochemical characteristics to *in vivo* aspects

Samuli Hirsjärvi[a1*], Sandrine Dufort[b1], Guillaume Bastiat[a], Patrick Saulnier[a], Catherine Passirani[a], Jean-Luc Coll[b], Jean-Pierre Benoît[a]

[a] LUNAM Université, Université d'Angers, INSERM U1066, IBS-CHU Angers, 4 rue Larrey, 49933 Angers, France

[b] INSERM-UJF-CRI-U823, Institut Albert Bonniot, 38706 La Tronche, France

[1] Equal contribution

[*] *Corresponding author* (S. Hirsjärvi): samuli.hirsjarvi@univ-angers.fr, tel.: +33 2 44 68 85 45; fax: +33 2 44 68 85 46.

Abstract

Attachment of polysaccharides on the surface of nanoparticles offers possibility to modify physicochemical and biological properties of the core particles. Surface of lipid nanocapsules (LNC) was modified by post-insertion of amphiphilic lipochitosan (LC) or lipodextran (LD). Modelling of these LNC by drop tensiometer technique revealed that the positively charged LC made the LNC surface more rigid whereas the neutral, higher M_W LD had no effect on the surface elasticity. Both LNC-LC and LNC-LD activated more the complement system than the blank LNC, thus proposing increased capture by the mononuclear phagocyte system (MPS). *In vitro*, the positively charged LNC-LC were more efficiently bound by the model HEK293(β_3) cells compared to LNC and LNC-LD. Finally, it was observed that neither LC nor LD did change *in vivo* biodistribution properties of LNC in mice. These polysaccharide-coated LNC, especially LNC-LC, are promising templates for targeting ligands (*e.g.* peptides, proteins) or therapeutic molecules (*e.g.* siRNA).

Keywords: lipid nanocapsules, post-insertion, polysaccharides, drop tensiometer, cellular uptake, biodistribution

1 Introduction

Research on nanoparticles since the latest decades has resulted in drug delivery systems that protect the active substance, improve solubility, and deliver the drug to specific tissular, cellular or molecular targets in the body [1].

Lipid nanocapsules (LNC), with tuneable size between 20-100 nm, are biomimetic synthetic nanocarriers used in drug delivery and imaging [2]. LNC consist of low-toxicity materials (PEGylated surfactant, lecithin, triglycerides) and their fabrication, a low-energy organic solvent-free phase inversion process, can be easily scaled up. Because of their semi-rigid shell, LNC can be modified by post-insertion of amphiphilic molecules. This kind of insertion allows *e.g.* improvement of biodistribution profile [3] or creation of templates for further attachment of targeting ligands [4, 5].

Besides nanoparticles consisting solely of polysaccharide [6], polysaccharides as a surface material of polymer or lipid nanoparticles are used to alter biological behaviour or serve as targeting moieties or templates for further functionalization [7]. For example, mannose-coated polymer nanoparticles and liposomes have been studied in targeting the immune system [8, 9]. Positively charged chitosan on the nanoparticle surface offers possibility to attach negatively charged molecules (such as siRNA) by electrostatic interactions [10, 11]. Chitosan is also used to improve mucoadhesive properties of nanoparticles [12]. Probably the most studied application of polysaccharides within nanoparticles is the avoidance of rapid particle clearance by the mononuclear phagocyte system (MPS) after opsonisation. Depending on their conformation on the nanoparticle surface, dextran, chitosan and heparin can reduce complement activation induced by the particles [13, 14]. A combination of chitosan and PEG on polymer nanoparticles reduced

macrophage uptake and prolonged blood circulation time significantly when compared to “classic” PEGylated nanoparticles [15].

Apart from size, surface charge and hydrophilicity, elasticity and shape are less studied parameters that can have a profound influence on the nanoparticle fate *in vivo* [16-18]. In fact, elasticity is reported to have an effect on the biodistribution and membrane passing capacity of nanoparticles [19, 20]. It is also considered as an important factor in the evaluation of toxicology of nanomaterials [21]. Elasticity might also be related to the mobility of the molecular chains on the nanoparticle surface, thus affecting the uptake by the MPS [22]. It has been observed that the LNC structure exhibits certain elasticity and deformability which depends on the particle size [23-25]. Drop tensiometer, a technique used to study rheology of different bio-related interfaces [26-28], can be used as a tool to address the elasticity evaluation.

In this study, two polysaccharides were post-inserted in the LNC shell: positively charged lipochitosan (LC, 5 kDa) [11] or bulky lipodextran (LD, 40 kDa) [29]. Effect of these polysaccharides on the elasticity of LNC was first evaluated by analysing LNC-mimicking oil drops using a drop tensiometer. Then, the capacity of LNC to avoid MPS clearance was assessed by an *in vitro* complement activation assay. In addition to these evaluations, *in vitro* uptake of the surface-modified LNC by model tumor cells, HEK293(β_3) originating from a human embryonic kidney cell line, was tested followed by determination of their *in vivo* fate in *nude* mice bearing the same subcutaneous xenografts.

The principal aims of this study were to evaluate how the drop tensiometer technique could be used in the modelling and characterization of elasticity of post-inserted semi-solid nanoparticles, and, on

the other hand, does the surface modification of LNC by polysaccharides affect their biological behaviour such as stealthiness.

2 Materials and Methods

2.1 Materials

Solutol® HS15 (PEG 660 12-hydroxystearate, M_W 870 Da) (BASF, Ludwigshafen, Germany), Labrafac® WL 1349 (caprylic/capric acid triglycerides) (Gattefossé S.A., Saint-Priest, France), Lipoid® S75-3 (Lipoid GmbH, Ludwigshafen, Germany), NaCl (Prolabo VWR International, Fontenay-sous-Bois, France) and MilliQ185 water (Waters, Saint-Quentin-en-Yveline, France) were used in the LNC preparation. Chitosan oligosaccharide lactate coupled to stearic anhydride (lipochitosan, LC, M_W 5 kDa) [11] and dextran coupled to amphiphilic hydroxylamine (lipodextran, LD, M_W 40 kDa) [29] were synthesised as described in the reported references. 1,1'-dioctadecyl-3,3,3',3'-tetramethylindodicarbocyanine perchlorate (DiD) was from Invitrogen (Cergy-Pontoise, France). Cibacron brilliant red 3B-A and anthrone reagent were from Sigma-Aldrich (Steinheim, Germany). All other used reagents were of analytical grade.

2.2 Methods

2.2.1 LNC preparation, post-insertion and characterization

LNC were prepared by the phase inversion temperature method described by Heurtault *et al.* [30]. Briefly, a mixture of Solutol® (282 mg), Lipoid® (25 mg), Labrafac® (343 mg), NaCl (30 mg) and water (987 mg) was subjected to three 65 °C ↔ 85 °C temperature cycles. During the last decrease

of temperature, at 78 °C (within the phase inversion zone), the system was diluted with cold (4 °C) water (4.2 mL) leading to formation of stable LNC. Fluorescent dye (DiD) was dissolved in acetone and added in the LNC preparation vial. Acetone was evaporated before addition of the components of the LNC. Final concentration of DiD was 2 mmol/L of Labrafac®. Encapsulation of the dye was verified by vortexing equal volumes (500 µL) of LNC dispersion (DiD encapsulated) (aqueous phase) and Labrafac® (oily phase) together followed by centrifugation (10 000 rpm, 45 min) and analysis of fluorescence of both phases (Fluoroskan Ascent reader, Thermo Fisher Scientific, Saint Herblain, France). This experiment assessed possible diffusion of the dye into Labrafac®.

To perform a post-insertion, LNC were incubated with LC or LD with stirring at 60 °C for 2 h (Fig. 1). An excess of the amphiphilic molecules *vs.* LNC was used: ~20 mol-% of the Solutol® and Lipoid® amount [31]. The post-inserted LNC were dialysed (Spectra/Por regenerated cellulose membranes with 50 kDa molecular weight cut-off, Spectrum Laboratories, Inc., Breda, The Netherlands) overnight against excess water.

Outcome of the surface modification was verified by size and ζ-potential measurements (Zetasizer ZS, Malvern, Worcestershire, UK). Particle sizing was based on photon correlation spectroscopy (PCS); the results were analyzed by CONTIN algorithm and the sizes were presented based on the volume distributions together with polydispersity indices (PdI). Electrophoretic mobilities were converted to ζ-potentials using Smoluchowski's equation.

2.2.2 Determination of the post-inserted quantities

The inserted quantities were assayed by colorimetric methods. Post-inserted LNC samples in water were centrifuged at 1 000 000 *g* for 1 h with a Beckman Coulter Optima™ MAX-XP

Ultracentrifuge (Brea, CA). After centrifugation, LNC deposited on the surface (LNC density was lower than the medium density) and the medium were removed, and the pellet composed of the non-inserted molecules was analysed and compared to corresponding established calibration curves.

LC was assayed by a method adapted from Muzzarelli [32]. A calibration curve was established by adding 3 mL of 75 µg/mL Cibacron brilliant red 3B-A solution (in water) in 300 µL LC solutions (in water) with final concentrations from 0 to 15 µg/mL. The pellet from centrifugation was then analysed with the help of the dye in the same way. Spectrophotometric analysis was performed at 575 nm against water with Uvikon 922 spectrophotometer (Kontron Instruments, Montigny-Le-Bretonneux, France).

LD was assayed with anthrone reagent [33]. In an ice bath, two parts anthrone reagent (50 mg anthrone in 25 mL *conc.* H_2SO_4) was added to one part of lipodextran pellet resuspended in water. Then, the sample tubes were placed in boiling water bath for 13 min. The tubes were cooled down in an ice bath, and kept at room temperature for 30 min before analysis at 620 nm with spectrophotometer. The LD concentration assay by this method was found to be linear from 0 to 200 µg/mL.

2.2.3 Drop tensiometer study

Drop tensiometer evaluation with Tracker equipment (ITConcept, Longessaigne, France) was performed as described in a previous study [34]. Briefly, a 5 µL rising drop of Labrafrac® (containing Lipoid®), mimicking an LNC, was formed using a microsyringe and a gauge into a glass vial filled with water (containing Solutol®). The axial symmetric shape (Laplacian profile) of the drop was analyzed using a camera. With Laplace's equation integration of the drop profile, the

interfacial tension and surface area could be simultaneously calculated and recorded. In order to adsorb Lipoid® and Solutol® in the interface, the drop was equilibrated for 16 h (at 25 °C) keeping the surface area constant. At the end of the equilibration time, equilibrium surface tension was registered. The drop was subjected to harmonic (sinusoidal) surface area alterations (amplitude of the sinusoids 0.3 µL). Periods (pulsations, ω) of the sinusoids ranged from 3 to 300 s corresponding to a rad/s range 2.09-0.02. Alterations in surface tension for each pulsation were treated by a harmonic analysis (Windrop software, ITConcept, Longessaigne, France) that allowed calculation of the parameters G' (elasticity real part) and G'' (elasticity imaginary part) [35]. From the presentation of G' and G''/ω as a function of ω, the rheological parameters E_e (elastic component; long range organization of the interface and the interactions between the interfacial molecules), E_{ne} (dissipative component; molecular interactions between the amphiphilic molecules and the aqueous or the lipophilic phase), and τ (relaxation time; time of the interface to reach a new equilibrium energetic state after a perturbation) were optimized by a simulated annealing method [34].

Concentrations of Solutol® in the aqueous phase and Lipoid® in the oil drop were adjusted to give the same theoretical proportion in the surface of the 5 µL drop as in the surface of LNC, namely 91% Solutol® and 9% Lipoid® [34]. To simulate the surface modification, a part of Solutol® in the water phase was replaced by LC or LD at the same mol-% as was observed to be inserted on the LNC surface. Another tested mol-%, 50%/50% inserted molecule/Solutol®, allowed better comparison between LC and LD.

2.2.4 Complement activation evaluation

Complement consumption was analysed in normal human serum (NHS) (provided by the Établissement Français du Sang, Angers, France) by measuring the residual haemolytic capacity of

the complement system after contact with the LNC. Poly(methyl methacrylate) (PMMA) nanoparticles were used as a positive control (strong complement activators) [14]. The technique is described in detail elsewhere [36]. Briefly, the amount of serum able to lyse 50% of a fixed number of sheep erythrocytes (CH50) (previously sensitized by rabbit antisheep erythrocyte antibodies), is determined. Complement activation was expressed as a function of the LNC surface area. Nanoparticle surface areas were calculated using the equation: $S = n4\pi r^2$ and $V = n(4/3)(\pi r^3)$ leading to $S = 3m/r\rho$, where S was the surface area (cm^2) and V the volume (cm^3) of n spherical particles of average radius r (cm), m the weight (µg) and ρ the volumetric mass (µg/cm^3) [14]. All these experiments were performed in triplicate.

2.2.5 LNC uptake by HEK293(β_3) cells

HEK293(β_3), stable transfectants of human β_3 from the human embryonic kidney cell line (kindly provided by J-F. Gourvest, Aventis, France), were cultured in DMEM supplemented with 1% glutamine and 10% FBS (Lonza, Verviers, Belgium), 50 units/mL penicillin, 50 µg/mL streptomycin (Sigma, Saint-Quentin Fallavier, France), and 700 µg/mL geneticin (G418 sulfate, Gibco, Paisley, UK). The cells were detached with trypsine and 1×10^6 cells were incubated 30 min with 57.5 µg of DiD-labelled LNC, LNC-LC or LNC-LD at 4 °C or 37 °C. Finally, the cells were washed twice with DPBS, centrifuged, re-suspended, and analyzed by FACS (LSR II, Becton Dickinson, San Jose, CA). The results are presented as counts of cells as a function of DiD fluorescence intensity. Experiments were performed in triplicate.

2.2.6 In vivo biodistribution

In vivo behavior of LNC was tested in *nude* mice bearing HEK293(β_3) xenografts in their right flank (n=6/group). Female NMRI *nude* mice (6-8 weeks, Janvier, Le Genest-Saint-Isle, France) were injected subcutaneously with 1×10^7 HEK293(β_3) cells / mouse. After tumor growth (6 weeks), anesthetized mice (isoflurane/oxygen 3.5/4% for induction and 1.5/2% thereafter; CSP, Cournon, France) were injected in the tail vein by 200 µL dispersion of DiD-labelled LNC, LNC-LC or LNC-LD. Fluorescence images were acquired by a back-thinned CCD camera (ORCAII-BT-512G, Hamamatsu, Massy, France). The amount of injected particles was standardized and equalized according to their fluorescence intensity in order to inject the same amount of the DiD dye. After the imaging at 24 h, the mice were sacrificed and dissected in order to image the organs and analyze the plasma. Image display and analysis were performed using Wasabi software (Hamamastsu, Massy, France). Semi-quantitative data were obtained by drawing regions of interest (ROI) around each organ. All procedures and experimental protocols were approved by the ethical committee of Grenoble (France) for the use of animal research.

2.2.7 Statistical analysis

Statistical significance was determined by 2-tailed unpaired Student's *t*-test (when two variables) or by one-way ANOVA with Dunnett's test (when compared to a reference) (Prism, GraphPad Software, Inc., La Jolla, CA). The differences were considered as significant with $p < 0.05$.

3 Results

3.1 LNC preparation and post-insertion

Size and ζ-potential of the different LNC as well as the detected post-inserted LC and LD quantities are presented in Table 1. All three LNC types (LNC, LNC-LC, LNC-LD) presented homogeneous size distributions (low polydispersity indices, PdI). Sizes of the post-inserted LNC were significantly higher than the size of blank LNC. Slightly negative ζ-potential of blank LNC (and LNC-LD) is assumed to originate from PEG groups forming dipoles able to interact with counter ions or water dipoles [37]. Positive ζ-potential of LNC-LC originated from amino groups of chitosan. In the evaluation of DiD diffusion into an added Labrafac® phase, neither fluorescence decrease in LNC (96.9±3.2% of the initial fluorescence after centrifugation) nor fluorescence apparition in the oil were observed indicating successful encapsulation of the dye. Additionally, PCS analysis of LNC before and after vortexing/centrifugation revealed identical particle sizes and count rate values. Similar count rate values indicated same LNC concentration (no particle disintegration during the analysis).

3.2 Drop tensiometer study

Equilibrium interfacial tensions (γ) together with the rheological parameters E_e, E_{ne} and τ are presented in Table 2. At constant temperature and pressure, γ equals Gibbs free energy (ΔG) per surface area. Therefore, because γ increased as a result of the interface modification by LC and LD, these interfaces became energetically less stable and less structured. Increase in E_e stands for increasing elasticity whereas increase in E_{ne} is a sign of rigidity but molecules can leave the interface more easily after a perturbation [23, 35]. Only the higher LD concentration (50%)

increased elasticity/fluidity of the interface (E_e increase). LC made the interface more rigid (E_{ne} increase). LC increased τ significantly, which meant longer equilibration time after a perturbation. Also LD increased τ and, thus, these values supported the increases in γ. Increase in the ratio E_e/E_{ne} can be considered to reflect more stable and, on the other hand, more fluid interface. Following E_e/E_{ne} ratios – presented here in an ascending order – were calculated: LC 15% 0.7; LC 50% 0.7; Solutol 100% 1.0; LD 5% 1.1; LD 50% 1.6.

3.3 Complement activation evaluation

Complement consumption was evaluated as the lytic capacity of the serum towards 50% of antibody-sensitized sheep erythrocytes (CH50 units) after exposure to different LNC (Fig. 2). PMMA nanoparticles (150 nm), as an assumed highly complement-activating control (*e.g.* no PEGylation) were included in the analyses. Indeed, they consumed already 73% of the CH50 units at 1 700 cm^2/ml. Instead, the tested LNC activated less the complement. At low surface areas, up to ~1 000 cm^2/mL, the activation profiles of LNC were identical. The lowest activation profile was registered for blank LNC; the two surface-modified LNC formulations were higher activators than blank LNC (LNC-LC starting from 1 000 cm^2/mL, LNC-LD from 2 200 cm^2/mL). LNC-LC consumed slightly more complement, throughout the tested concentration range, when compared to LNC-LD. *E.g.* at ~5 100 cm^2/mL, consumption values were 28, 48 and 59% for LNC, LNC-LD and LNC-LC, respectively.

3.4 LNC uptake by HEK293(β_3) cells

Interactions of the different LNC with HEK293(β_3) cells were investigated *in vitro* by flow cytometry after incubation at 4 °C (binding) and 37 °C (internalization) (Fig. 3). After incubation at

37 °C, LNC and LNC-LD were weakly internalized by the cells, but the intensities of fluorescence remained under the positive cut-off value (vertical line) indicating a weak staining (no statistically significant difference between LNC and LNC-LD). On the contrary, LNC-LC interacted strongly with cells. Similar results of binding were obtained after incubation at 4 °C showing that no differences could be found between binding and internalization. Considering that the lipophilic DiD dye was encapsulated in the oily core of LNC, the attractive electrostatic interaction between the positively charged LC and the negatively charged surface of HEK293(β_3) cells demonstrated that LC remained attached to the LNC surface and that the particles were also in contact with the cells.

3.5 In vivo biodistribution

LNC, LNC-LC and LNC-LD were homogeneously distributed in mice after intravenous injections with a pronounced accumulation in the liver (Fig. 4) throughout the imaging time points and until the 24 h sacrifice. No significant differences were observed between the three formulations. Measurements of fluorescence in the plasma evidenced that these LNC still remained in the blood circulation after 24 h. A weak accumulation was observed in the skin (whole-body images and quantifications). Tumor accumulation was weak in the HEK293(β_3) model but the intensity of staining in the cervical lymph node was in the same range than in the liver. This lymph node was not located on the tumor side of the mouse, which suggested that the particle accumulation in the lymph node was not due to tumor drainage.

4 Discussion

The post-insertion technique has been originally developed for PEGylation and incorporation of targeting molecules on liposome surface [38]. A temperature rise enables a transfer between

phospholipids of the surface and the amphiphilic molecules from the aqueous environment. In the case of LNCs, the incorporation of amphiphilic molecules is rather controlled by the conformation of the PEG chains (Solutol®) which is more favourable at an elevated temperature: the ‘‘brush” conformation marked by the increased flexibility allow better penetration of the amphiphilic molecules between the PEG chains [39].

Increase in size and in ζ-potential (in the case of LNC-LC) confirmed the success of surface modification of LNC. Post-inserted quantities, 15% for LNC-LC and 5% for LNC-LD, were in line with previous studies where 12% LC [11], 7% DSPE-PEG_{2000}-maleimide [39], and 12% DSPE-PEG_{2000}-amino [40] were detected on the LNC surface. In the first study presenting the LD insertion on the LNC surface, 10% LD / LNC mass was detected after integration of the NMR signal [29]. The difference with the current study (5%) originated probably from the different detection method used (here: a colorimetric method). However, at a certain point during the post-insertion process, the density of molecular chains at the surface creates a steric barrier imbedding further post-insertion and, thus, limits the inserted quantity to 10-20% [41].

In the tensiometry evaluation, the less elastic nature of the oil drops containing LC originated probably from the electrostatic repulsion between the chitosan groups on the interface. Low ionic strength of the external medium (water) did not screen the positive charges of the NH_2 groups. This could be seen as an increase in E_{ne}, which meant that, upon perturbation, LC molecules were more prone to leave the interface. On the contrary, non-charged LD molecules on the interface could contribute only to steric repulsion upon interfacial perturbations (drop volume alterations). Generally, the effect of electrostatic repulsion extends to a longer distance than the effect of steric repulsion [42]. Indeed, LD did not notably change interfacial elasticity compared to Solutol®. It seemed that the electric charges (LC) had more effect on the interface than the molecule size (bulky

LD). These studies performed with oil-water interfaces let us assume that 15% post-inserted LC made the LNC surface more rigid whereas 5% LD had no effect on the LNC elasticity.

Density, length and conformation of the molecular chains (*e.g.* PEG, polysaccharides) on the nanoparticle surface have an influence on the uptake by the MPS and subsequently on the blood circulation time [22]. This can be evaluated by complement activation assays. When coupled to highly activating polymer nanoparticles, conformation of dextran ("loops and tails/brush") is reported to be determinant factor in reducing complement activation [13, 14, 43]. Dextran or chitosan of the same molecular weight on the surface of poly(ethylcyanoacrylate) nanoparticles have resulted in similar inhibition of the complement activation [13]. On the other hand, NH_2 groups of chitosan as well as OH groups (chitosan, dextran) are also known to be complement activators [44, 45].

In previous studies, LNC size increase from 25 to 50 and 100 nm had resulted in an increase of the complement activation profile [36] and also in a more rigid LNC surface [34]. Therefore, in the current study, taking into account that LNC with PEG (Solutol®) on their surface were low complement activators as such, and the size of LNC (49 nm) was increased as result of the post-insertion of LC (58 nm) and LD (62 nm), a probable reason for the higher complement activation observed with LNC-LC and LNC-LD originated from the size difference together with the possibly less elastic structure (in the case of LNC-LC). Also, the complement activating NH_2 and OH groups of LNC-LC and LNC-LD might have contributed to the higher CH50 unit consumption. Finally, the *in vivo* injected LNC quantity corresponded to about 4 000 cm^2/mL which means that at that particle surface area, LNC-LC and LNC-LD consumed about 15-20 %-points more CH50 units than the blank LNC. Therefore, these findings suggested that the post-inserted LC and LD could have an

effect on the LNC biodistribution, and especially a negative influence on the LNC blood circulation time.

In vitro, indeed, the attractive electrostatic interaction between the positively charged LNC-LC and the (negatively charged) surface of HEK293(β_3) cells was observed. However, this stronger binding did not promote internalization of LNC by these cells. Contrary to what could have been expected from the *in vitro* results, LNC-LC did not provide enhanced tumor retention *in vivo*. This might have been due to the nature of the HEK293(β_3) xenografts which are known to have well-structured, neo-angiogenic vasculature with tight endothelial junctions resulting in a weak EPR (enhanced permeability and retention) effect and, thus, low tumor accumulation of nanoparticles [46]. Our interest in using the HEK293(β_3) model derives from its overexpression of $\alpha_v\beta_3$ integrin, making it a potential target for RGD-peptide decorated LNC in further studies [47]. No effect on the *in vivo* LNC biodistribution in different organs was observed after the surface modification by LC or LD. These observed similar biodistribution profiles might have resulted from the fact that LNC without surface modification already possessed a stealth biodistribution profile that could not be improved by these amphiphilic molecules, LC or LD, on the surface. On the contrary, when the PEG chain length on the LNC surface was increased from 660 Da (Solutol®) to 2 000 Da, blood circulation time could be prolonged [3]. However, if the surface properties are otherwise similar (*e.g.* hydrophilic nature), other studies have also suggested that nanoparticle biodistribution (in the RES organs) is rather governed by the particle size than the surface properties such as ζ-potential [48]. In the current study, indeed, the particle sizes of LNC, LNC-LC and LNC-LD were similar (all within ~15 nm). Instead, chitosan added to the surface of quickly eliminated polymer nanoparticles significantly modified their biodistribution profile due to a resulting longer blood circulation time [49].

5 Conclusions

The results showed that the drop tensiometer technique could be used to evaluate how surface modification of LNC affected their elasticity. LC made the LNC-mimicking oil-water interface more rigid whereas LD seemed to provide elasticity. This difference was assumed to result from the electrically charged LC molecules. This technique could be applied in the studies of other semi-solid nanoparticles such as liposomes, or nanoemulsions. Information of nanoparticle elasticity together with other physicochemical characteristics might be useful when behaviour of nanoparticles at biological interfaces (*e.g.* membrane passage) is assessed. Surface modification of LNC by LC or LD did produce neither enhancing nor deteriorating effect on the LNC biodistribution and pharmacokinetics. This was a rather promising result, especially in the case of LC, because these LNC could be further functionalized by negatively charged pharmaceutically active molecules such as siRNA or proteins/peptides for active targeting.

Acknowledgements

Ms. Johanna Gutensohn is acknowledged for technical assistance. Plateau technique de synthèse organique de l'Axe Vectorisation & Radiothérapies, Cancéropôle Grand Ouest (France), is acknowledged for the synthesis of lipochitosan. Alexandre Barras (UMR 8161 CNRS Université de Lille, France) is acknowledged for the synthesis of lipodextran. This work was financially supported by the French National Research Agency (ANR) in the frame of its programme in Nanosciences and Nanotechnologies (CALIF project no. ANR-08-NANO-006).

References

1. Farokhzad OC, Langer R. Impact of nanotechnology on drug delivery. ACS Nano 2009;3:16-20.

2. Huynh NT, Passirani C, Saulnier P, Benoit JP. Lipid nanocapsules: A new platform for nanomedicine. Int J Pharm 2009;379:201-209.

3. Morille M, et al. Long-circulating DNA lipid nanocapsules as new vector for passive tumor targeting. Biomaterials 2010;31:321-329.

4. Béduneau A, Hindré F, Clavreul A, Leroux J-C, Saulnier P, Benoit J-P. Brain targeting using novel lipid nanovectors. J Control Release 2008;126:44-49.

5. Bourseau-Guilmain E, et al. Development and characterization of immuno-nanocarriers targeting the cancer stem cell marker AC133. Int J Pharm 2012;423:93-101.

6. Liu Z, Jiao Y, Wang Y, Zhou C, Zhang Z. Polysaccharides-based nanoparticles as drug delivery systems. Adv Drug Deliv Rev 2008;60:1650-1662.

7. Lemarchand C, Gref R, Couvreur P. Polysaccharide-decorated nanoparticles. Eur J Pharm Biopharm 2004;58:327-341.

8. Rieger J, Freichels H, Imberty A, Putaux J-L, Delair T, Jérôme C, Auzély-Velty R. Polyester nanoparticles presenting mannose residues: toward the development of new vaccine delivery systems combining biodegradability and targeting properties. Biomacromolecules 2009;10:651-657.

9. White KL, Rades T, Furneaux RH, Tyler PC, Hook S. Mannosylated liposomes as antigen delivery vehicles for targeting to dendritic cells. J Pharm Pharmacol 2006;58:729-737.

10. Pillé J-Y, et al. Intravenous delivery of anti-RhoA small interfering RNA loaded in nanoparticles of chitosan in mice: safety and efficacy in xenografted aggressive breast cancer. Human Gene Ther 2006;17:1019-1026.

11. Hirsjärvi S, Qiao Y, Royère A, Bibette J, Benoit J-P. Layer-by-layer surface modification of lipid nanocapsules. Eur J Pharm Biopharm 2010;76:200-207.

12. Mazzarino L, Travelet C, Ortega-Murillo S, Otsuka I, Pignot-Paintrand I, Lemos-Senna E, Borsali R. Elaboration of chitosan-coated nanoparticles loaded with curcumin for mucoadhesive applications. J Colloid Interface Sci 2012;370:58-66.

13. Bertholon I, Vauthier C, Labarre D. Complement activation by core-shell poly(isobutylcyanoacrylate)-polysaccharide nanoparticles: Influences of surface morphology, length, and type of polysaccharide. Pharm Res 2006;23:1313-1323.

14. Passirani C, Barratt G, Devissaguet J-P, Labarre D. Interactions of nanoparticles bearing heparin or dextran covalently bound to poly(methyl methacrylate) with the complement system. Life Sci 1998;62:775-785.

15. Sheng Y, et al. Long-circulating polymeric nanoparticles bearing a combinatorial coating of PEG and water-soluble chitosan. Biomaterials 2009;30:2340-2348.

16. Perry JL, Herlihy KP, Napier ME, DeSimone JM. PRINT: A novel platform toward shape and size specific nanoparticle theranostics. Accounts Chem Res 2011;44:990-998.

17. Decuzzi P, Godin B, Tanaka T, Lee SY, Chiappini C, Liu X, Ferrari M. Size and shape effects in the biodistribution of intravascularly injected particles. J Control Release 2010;141:320-327.

18. Longmire MR, Ogawa M, Choyke PL, Kobayashi H. Biologically optimized nanosized molecules and particles: More than just size. Bioconjugate Chem 2011;22:993-1000.

19. Arkhangelsky E, Sefi Y, Hajaj B, Rothenberg G, Gitis V. Kinetics and mechanism of plasmid DNA penetration through nanopores. J Membrane Sci 2011;371:45-51.

20. Christian DA, Cai S, Garbuzenko OB, Harada T, Zajac AL, Minko T, Discher DE. Flexible filaments for *in vivo* imaging and delivery: Persistent circulation of filomicelles opens the dosage window for sustained tumor shrinkage. Mol Pharm 2009;6:1343-1352.

21. Elsaesser A, Howard CV. Toxicology of nanoparticles. Adv Drug Deliver Rev 2012;64:129-137.

22. Vonarbourg A, Passirani C, Saulnier P, Benoit J-P. Parameters influencing the stealthiness of colloidal drug delivery systems. Biomaterials 2006;27:4356-4373.

23. Heurtault B, Saulnier P, Pech B, Benoit JP, Proust JE. Interfacial stability of lipid nanocapsules. Colloid Surf B 2003;30:225-235.

24. Minkov I, Ivanova T, Panaiotov I, Proust J, Saulnier P. Reorganization of lipid nanocapsules at air-water interface: Part 2. Properties of the formed surface film. Colloid Surf B 2005;44:197-203.

25. Minkov I, Ivanova T, Panaiotov I, Proust J, Saulnier P. Reorganization of lipid nanocapsules at air-water interface I. Kinetics of surface film formation. Colloid Surf B 2005;45:14-23.

26. Kazakov VN, Fainerman VB, Kondratenko PG, Elin AF, Sinyachenko OV, Miller R. Dilational rheology of serum albumin and blood serum solutions as studied by oscillating drop tensiometry. Colloid Surf B 2008;62:77-82.

27. Li JB, Kretzschmar G, Miller R, Möhwald H. Viscoelasticity of phospholipid layers at different fluid interfaces. Colloid Surf A 1999;149:491-497.

28. Wüstneck R, Wüstneck N, Grigoriev DO, Pison U, Miller R. Stress relaxation behaviour of dipalmitoyl phosphatidylcholine monolayers spread on the surface of a pendant drop. Colloid Surf B 1999;15:275-288.

29. Richard A, Barras A, Younes AB, Monfilliette-Dupont N, Melnyk P. Minimal chemical modification of reductive end of dextran to produce an amphiphilic polysaccharide able to incorporate onto lipid nanocapsules. Bioconjugate Chem 2008;19:1491-1495.

30. Heurtault B, Saulnier P, Pech B, Venier-Julienne M-C, Proust J-E, Phan-Tan-Luu R, Benoit J-P. The influence of lipid nanocapsule composition on their size distribution. Eur J Pharm Sci 2003;18:55-61.

31. Perrier T, Saulnier P, Fouchet F, Lautram N, Benoit J-P. Post-insertion into lipid nanocapsules (LNCs): From experimental aspects to mechanisms. Int J Pharm 2010;396:204-209.

32. Muzzarelli RAA. Colorimetric determination of chitosan. Anal Biochem 1998;260:255-257.

33. Scott TA, Melvin EH. Determination of dextran with anthrone. Anal Chem 1953;25:1656-1661.

34. Hirsjärvi S, Bastiat G, Saulnier P, Benoit J-P. Evaluation of surface deformability of lipid nanocapsules by drop tensiometer technique, and its experimental assessment by dialysis and tangential flow filtration. Int J Pharm 2012;434:460-467.

35. Saulnier P, et al. Rheological model for the study of dilational properties of monolayers. Comportment of dipalmitoylphosphatidylcholine (DPPC) at the dichloromethane (DCM)/water interface under ramp type or sinusoidal perturbations. Langmuir 2001;17:8104-8111.

36. Vonarbourg A, Passirani C, Saulnier P, Simard P, Leroux J-C, Benoit JP. Evaluation of pegylated lipid nanocapsules versus complement system activation and macrophage uptake. J Biomed Mat Res A 2006;78A:620-628.

37. Vonarbourg A, Saulnier P, Passirani C, Benoit J-P. Electrokinetic properties of noncharged lipid nanocapsules: Influence of the dipolar distribution at the interface. Electrophoresis 2005;26:2066-2075.

38. Uster PS, Allen TM, Daniel BE, Mendez CJ, Newman MS, Zhu GZ. Insertion of poly(ethylene glycol) derivatized phospholipid into pre-formed liposomes results in prolonged in vivo circulation time. FEBS Lett 1996;386:243-246.

39. Béduneau A, Saulnier P, Hindré F, Clavreul A, Leroux J-C, Benoit J-P. Design of targeted lipid nanocapsules by conjugation of whole antibodies and antibody Fab' fragments. Biomaterials 2007;28:4978-4990.

40. Perrier T, Fouchet F, Bastiat G, Saulnier P, Benoit J-P. OPA quantification of amino groups at the surface of Lipidic NanoCapsules (LNCs) for ligand coupling improvement. Int J Pharm 2011;419:266-270.

41. Sou K, Endo T, Takeoka S, Tsuchida E. Poly(ethylene glycol)-modification of the phospholipid vesicles by using the spontaneous incorporation of poly(ethylene glycol)-lipid into the vesicles. Bioconjugate Chem 2000;11:372-379.

42. Florence AT, Attwood D. Physicochemical principles of pharmacy. 3rd ed. Houndmills: Palgrave; 1998.

43. Passirani C, Barratt G, Devissaguet J-P, Labarre D. Long-circulating nanoparticles bearing heparin or dextran covalently bound to poly(methyl methacrylate). Pharm Res 1998;15:1046-1050.

44. Suzuki Y, Miyatake K, Okamoto Y, Muraki E, Minami S. Influence of the chain length of chitosan on complement activation. Carbohydr Polym 2003;54:465-469.

45. Torchilin V, Papisov M. Why do polyethylene glycol-coated liposomes circulate so long?: Molecular mechanism of liposome steric protection with polyethylene glycol: Role of polymer chain flexibility. J Liposome Res 1994;14:725-739.

46. Jin Z-H, Josserand V, Foillard S, Boturyn D, Dumy P, Favrot M-C, Coll J-L. *In vivo* optical imaging of integrin α_v-β_3 in mice using multivalent or monovalent cRGD targeting vectors. Mol Cancer 2007;6:41.

47. Sugahara KN, et al. Tissue-penetrating delivery of compounds and nanoparticles into tumors. Cancer Cell 2009;16:510-520.

48. He C, Hu Y, Yin L, Tang C, Yin C. Effects of particle size and surface charge on cellular uptake and biodistribution of polymeric nanoparticles. Biomaterials 2010;31:3657-3666.

49. Kim J-Y, Choi WI, Kim YH, Tae G, Lee S-Y, Kim K, Kwon IC. *In-vivo* tumor targeting of pluronic-based nano-carriers. J Control Release 2010;147:109-117.

Figure captions

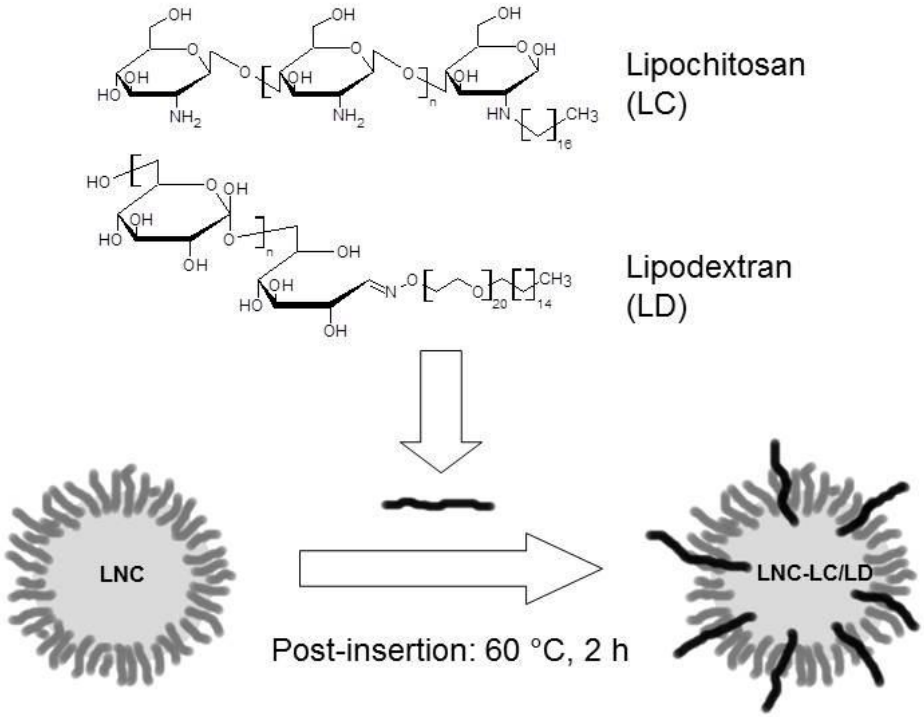

Figure 1. Chemical structures of lipochitosan (LC) and lipodextran (LD) post-inserted in the LNC shell. The shell consists of Solutol® and Lipoid® molecules, the oil core of medium chain length triglycerides (Labrafac®).

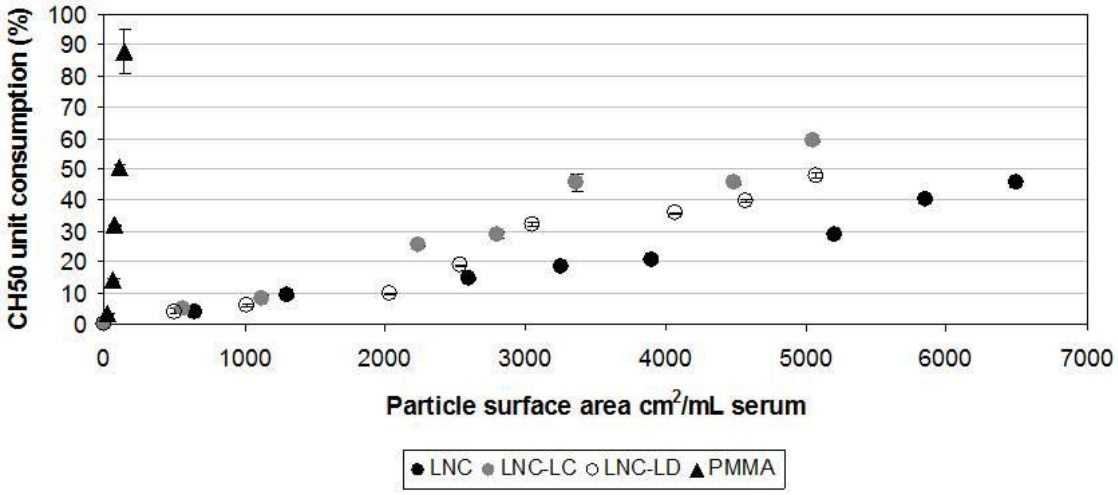

Figure 2. Complement consumption of LNC, LNC-LC and LNC-LD at 37 °C, 1 h. PMMA nanoparticles (150 nm) were used as a highly complement activating control.

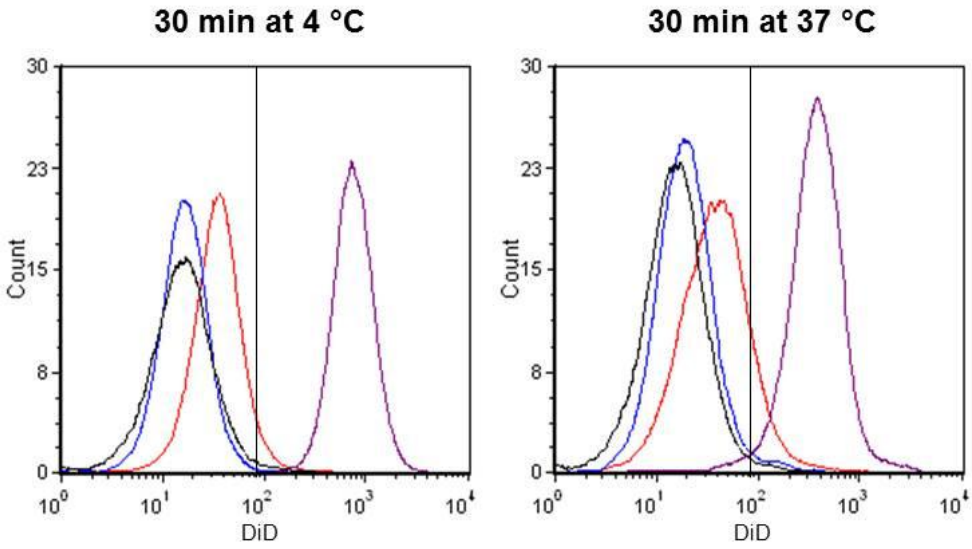

Figure 3. *In vitro* uptake of LNC (red), LNC-LC (purple) and LNC-LD (blue) by HEK293(β3) cells 30 min after incubation at 4 °C and 37 °C ([DiD] = 0.2 µM) (control cells in black).

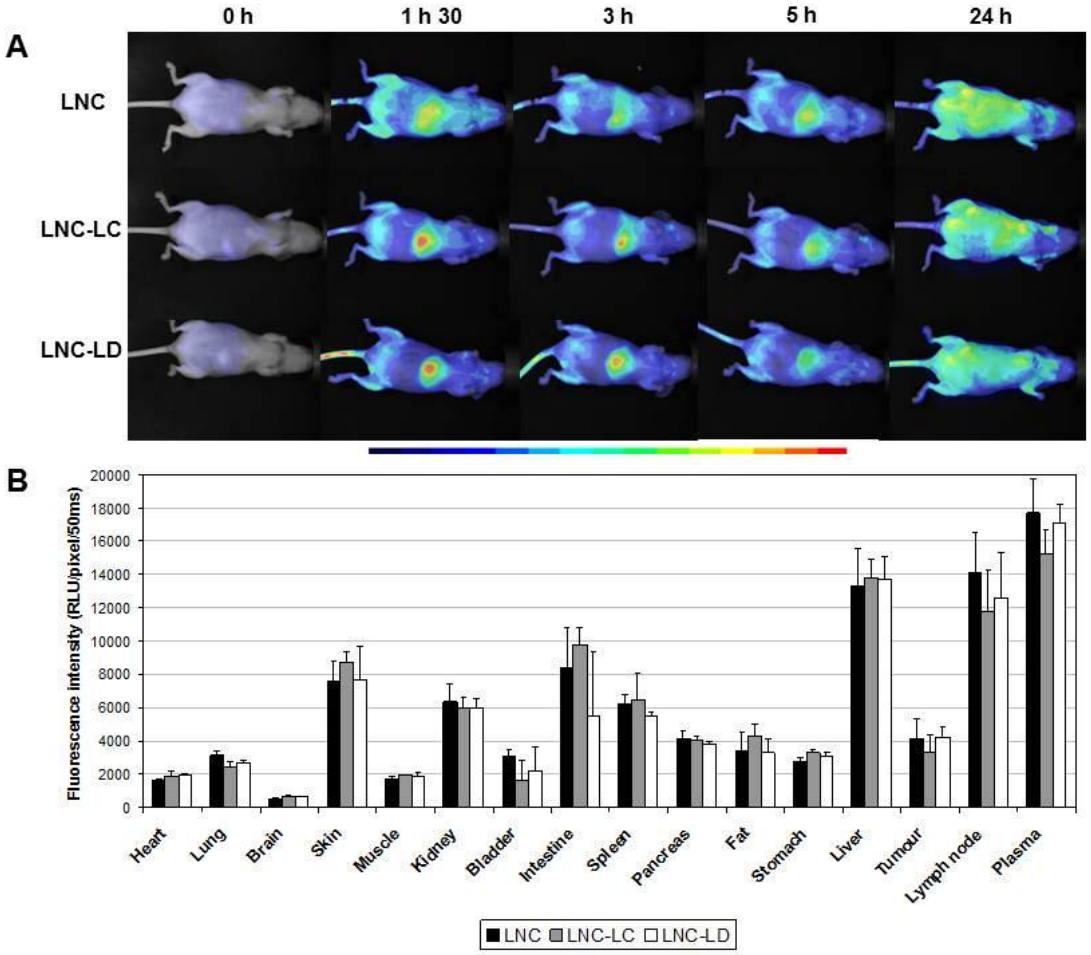

Figure 4. *In vivo* biodistribution of LNC, LNC-LC and LNC-LD in HEK293(β_3) xenografted *nude* mice. Fluorescence images (200 ms integration time, color scale) were recorded at different times after injection and superimposed to visible light images (white and black) (A). Quantification of the fluorescence signals of the different organs after dissection together with fluorescence of the plasma, 24 h after injection (B).